Hindawi
Advances in Civil Engineering
Volume 2023, Article ID 8828952, 12 pages
https://doi.org/10.1155/2023/8828952

Research Article

Freezing Damage Control of Railway Subgrade Miniature Shields in Cold Climatic Regions: Construction Technology Optimization via Numerical Simulation

Caolin Qing,[1,2] **Shaolong Jie**,[3] **Zurun Yue**,[1] **Liwei Wang**,[4] **and Bingcheng Wang**[4]

[1]*State Key Laboratory of Mechanical Behavior and System Safety of Traffic Engineering Structures, Shijiazhuang Tiedao University, Shijiazhuang 050043, China*
[2]*College of Civil Engineering, Shijiazhuang Tiedao University, Shijiazhuang 050043, China*
[3]*Shijiazhuang University, Shijiazhuang 050035, China*
[4]*Beijing Huatie Times Construction & Development Co. Ltd., Beijing 101300, China*

Correspondence should be addressed to Shaolong Jie; hebutjsl@163.com

Received 23 August 2023; Revised 7 October 2023; Accepted 11 October 2023; Published 6 November 2023

Academic Editor: Xing Wang

Microshield structure replacement technology is commonly used to control the freezing damage of railway roadbeds, featuring high efficiency and easy operation. However, improper disposal of measures in the construction process will still cause excessive deformation of the line and endanger the safety of train operations. On the background of a subgrade freezing damage improvement and speed improvement project of the Xige section of Quinghai–Tibet railway, this study performed numerical simulation of the microshield based on the measured data of the field automatic monitoring system to improve the operation safety of the existing lines and optimize the construction technology of the microshield. The effect of the changes in the microshield segment material, construction process, and formation loss on the settlement of the operating railway subgrade was analyzed to control the construction disturbance settlement of the existing operating line. The results obtained show that the overall settlement deformation of the line is small when the steel pipe is used as the shield segment, which meets the safety management requirements of the existing operating line. When PE tube segments are used for construction, construction measures should be strictly controlled to reduce the effect of settlement deformation on the operational lines. When steel pipe segments are used, the settlement generated by the construction process from both sides to the middle is minimal. When PE tube segments are adopted in the construction, the settlement generated by the construction process with unilateral advancement and an interval of two pipe diameters is the least, producing unimodal settlement curve of the line. The latter features a double peak when the shield pipe interval is three pipe diameters or more. When using PE tube pieces for the microshield construction, it is necessary to strictly control the formation loss rate within 10% by optimizing the construction control measures.

1. Introduction

With the increasing operating mileage of high-speed railways in multiple frozen soil areas of China [1], frost swelling deformation of railway roadbeds often occurs, affecting the line smoothness and safety of train running. A subgrade freezing damage improvement and speed improvement project of Xige section of Quinghai–Tibet railway (hereinafter referred to as Xige Line) aims to improve the overall smoothness of the line and provide a guarantee for the Fuxing" EMU online and railway safety operation. However, there are 1,207 local frost-heaving deformation locations on the Xige Line, and the frozen damage line is 59,220-m long [2]. The main causes of frost heave are as follows: it is close to Qinghai Lake, the groundwater level is high, the soil of the foundation bed is silty clay, and the water content is high [3]. Therefore, alleviating the over-limit deformation of the Xige Line caused by frost heave is very topical.

Many scholars have researched the treatment measures for frost-heaving deformation of railway roadbeds in the cold regions. Studying the temperature field of the coupling of water and heat, Tai et al. [4] proposed using an asphalt

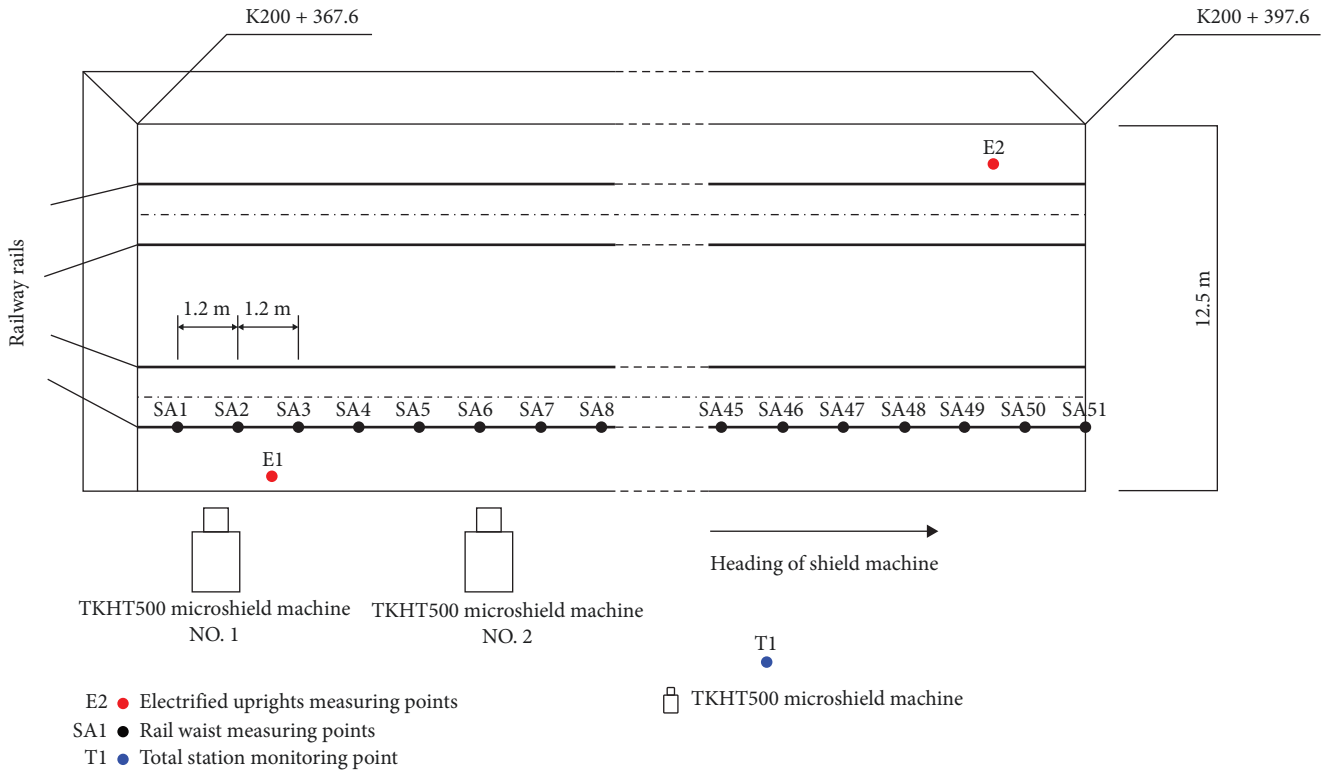

Figure 1: Construction situation and plan view of the measuring points.

concrete strengthened layer + cement stabilized gravel + thermal insulation board foundation structure to protect the roadbed from frost heave. Shen et al. [5] used graded gravel mixed with 3% cement as backfill in the transition section of roads and bridges to control the frost heave. These two methods are suitable for the initial stage of new railway construction. Hu et al. [6, 7] proposed an active heating device based on the solar energy and geothermal energy, while Li [8] introduced an "integrated" heating device for heating sections and heating collection sections based on a ground source heat pump. These two active protection methods are very effective, but their economy needs to be improved. Liu et al. [9] used fly ash and cement-based foam concrete mixed with silt on the surface of the foundation bed and slope as the subgrade thermal insulation strengthening layer. Yang [10] used the salt injection method to convert frost-heaving soil into the artificial saline soil and controlled frost-heaving and thawing settlement by limiting water transfer in the soil. These two passive protection methods still need to improve regarding the anti-frost heaving effect and durability. Yan [11] proposed the microshield targeted replacement technology, which can directly replace the bad subgrade fillers through the microshield replacement method, which can improve the subgrade fillers and reduce the frost heave sensitivity, and has achieved a good regulation effect in the Qinhuang–Shenyang passenger special line [12]. However, there is still room for improvement in the construction technology.

In this paper, based on the characteristics of the subgrade of the Xige Line, microshield replacement technology is used to control the construction disturbance settlement of existing operating lines and the effect of factors such as segment material, construction process, and formation loss on the settlement of railway subgrade is analyzed according to the field measured data. This paper puts forward the construction optimization measures of railway roadbed freezing damage rectification and replacement technology under specific working conditions, which is of great value for improving the treatment of frost-heave defects of existing railways in seasonally freezing areas in China.

2. Project Overview

2.1. Climatic and Geological Conditions of the Site. The construction site is located in the eastern section of the Xige section of Quinghai–Tibet railway. This section of the railway (hereinafter referred to as Xige Line) is a common line for the passengers and goods. The line starts from Xiaqiao Station in Xining City and ends in the Golmud City, passing through seven cities and counties, with a total length of about 763.2 km. The construction situation and plan view of the measuring points are shown in Figure 1. The Xige Line has a higher altitude and a longer duration of low temperature. Every year from late October to late March, the temperature in this section is below 0°C, and the lowest temperature can reach −20°C [3]. The Xige Line passes through the Qinghai Lake basin, with large temperature differences and abundant water resources, and the frost-heaving phenomenon is obvious during the autumn and winter seasons, which affects

Table 1: Physical index of bad subgrade soil.

Physical index	Parameter
Soil properties	Silty clay
Optimum moisture content (%)	20.68
Dry density (g/cm^3)	1.30
Maximum dry density (g/cm^3)	1.76
Liquid limit (%)	36.70
Plastic limit (%)	25.60
Plasticity index	11.0
Liquid index	1.5

train operation. According to the laboratory geotechnical tests on the subgrade of Signes section [13], the subgrade soil of Xige section of Qinghai–Tibet railway belongs to silty clay with low-liquid limit and low permeability. The mechanical properties of poor roadbed soil are shown in Table 1.

2.2. Construction Situation of the Microshield. The construction section line is the ballasted track. The width of the roadbed surface is 12 m, the thickness is 0.4 m, as shown in Figure 1(a), the roadbed thickness at the construction site shall be 2.1 m, and the portion of the undesirable soil shall be in the range of 0.4–m below the surface of the subgrade bed, the thickness is 500 mm and the bad roadbed filler to be replaced, and the horizontal filling depth is 6 m. The structure of the subgrade is shown in Figure 2. Two TKHT500 microshield machines with a segment diameter of 500 mm were configured on site. The two shield machines were separated by four times the pipe diameter, and the construction was carried out on one side. The whole construction process is as follows: first, the soil is excavated by the advanced bit, and the segments can be placed in every 1 m of excavation, and the segments are all placed in the subgrade soil when the depth is 6 m. After the excavation was inserted into the segments, the foam insulation board was inserted into the shield pipe, and concrete was used for grouting to replace the frost-heaving subgrade filler. Finally seal the pipe. To compare the effect of using steel pipe segments with PE tube segments, two working points with similar climate and temperature conditions were selected: upstream K237 + 940– K238 + 080, PE tube segments were used for construction, model SDR17, outer diameter of 500 mm, nominal wall thickness of 29.7 mm; downward K200 + 350–K200 + 430, the use of steel pipe segments for construction, model Q235, outer diameter of 500 mm, nominal wall thickness of 5 mm, the two construction processes were completely consistent. The actual measurement of this project began on August 10, 2022, and ended on November 10, 2022, for a total of 92 days. The PE tube and steel pipe used in the project are shown in Figure 3.

2.3. Physical and Mechanical Parameters of the Filler of the Base Bed. The physical and mechanical properties of subgrade packing and the compacting quality of subgrade packing were tested at the construction site. The physical properties of subgrade packing within the construction scope are listed in Table 2.

3. Field Monitoring

3.1. Monitoring Implementation Plan. The on-site settlement monitoring scheme comprised an automatic monitoring system and microprecision prism measurement technology [14]. A Leica TS60 total station and microprecision prism were used for automatic monitoring. A total of 101 measuring points were arranged in the rail waist of the construction point K237 + 940–K238 + 080, and two measuring points were electrified columns. The measuring interval was 60 min. Downward K200 + 350–K200 + 430 at the construction point of the rail waist arranged 51 measuring points, electrified column measuring points 2, with a measuring interval of 30 min. The distance between the measuring points at the rail waist is 1.2– 2.4 m, and the remaining parts were properly encrypted and laid according to actual needs. The layout position of the microprecision prism measuring points is shown in Figure 4.

3.2. Analysis of Actual Settlement Data. The monitoring work run through the whole process of excavation, shield tunneling, displacement, grouting, and backfilling. In addition to the automatic monitoring by the total station instrument, an SAA array displacement meter and manual track gauge were also used to measure the site. Fourteen reference points were used in the measuring test section to compare the monitoring data of the three methods, as shown in Figure 5. By comparison, the data of the total station automatic monitoring system were found to be accurate and reliable to be used as the basis for model analysis.

4. Simulation Model Establishment and Verification

4.1. Establishment of Miniature Shield Model. During the construction of the miniature shield, the size of the shield bit made of steel pipes differed from that made of the PE tubes. Soft material of the PE tubes made it easily deformed under the action of earth pressure during the insertion of the pipe segment, and the resistance was large, making it difficult to ensure normal construction. To reduce the friction resistance of the roadbed soil to the PE tube, 20-mm thick overdigging (OD) was adopted in the construction process. Therefore, this study focused on the use of steel pipes and PE tubes in the construction. The PE tube model considered the formation loss caused by OD and added the formation loss coefficient to the shield soil to simulate OD. However, the steel pipe material was hard enough to overcome the friction resistance of the subgrade soil when inserting the steel pipe, and there was no need to set the OD during the construction process, so the impact of formation loss was ignored. The construction difference between the two pipe segments is shown in Figure 6.

It was assumed that the soil quality of each layer of the subgrade section under construction was evenly distributed and belonged to the continuous body of equal sections. ABAQUS finite-element software was used for 3D modeling. The Mohr–Coulomb soil constitutive relation model was adopted, in which the basic body length of the road to be excavated was 30 m, the width was 12 m, the height was 5 m,

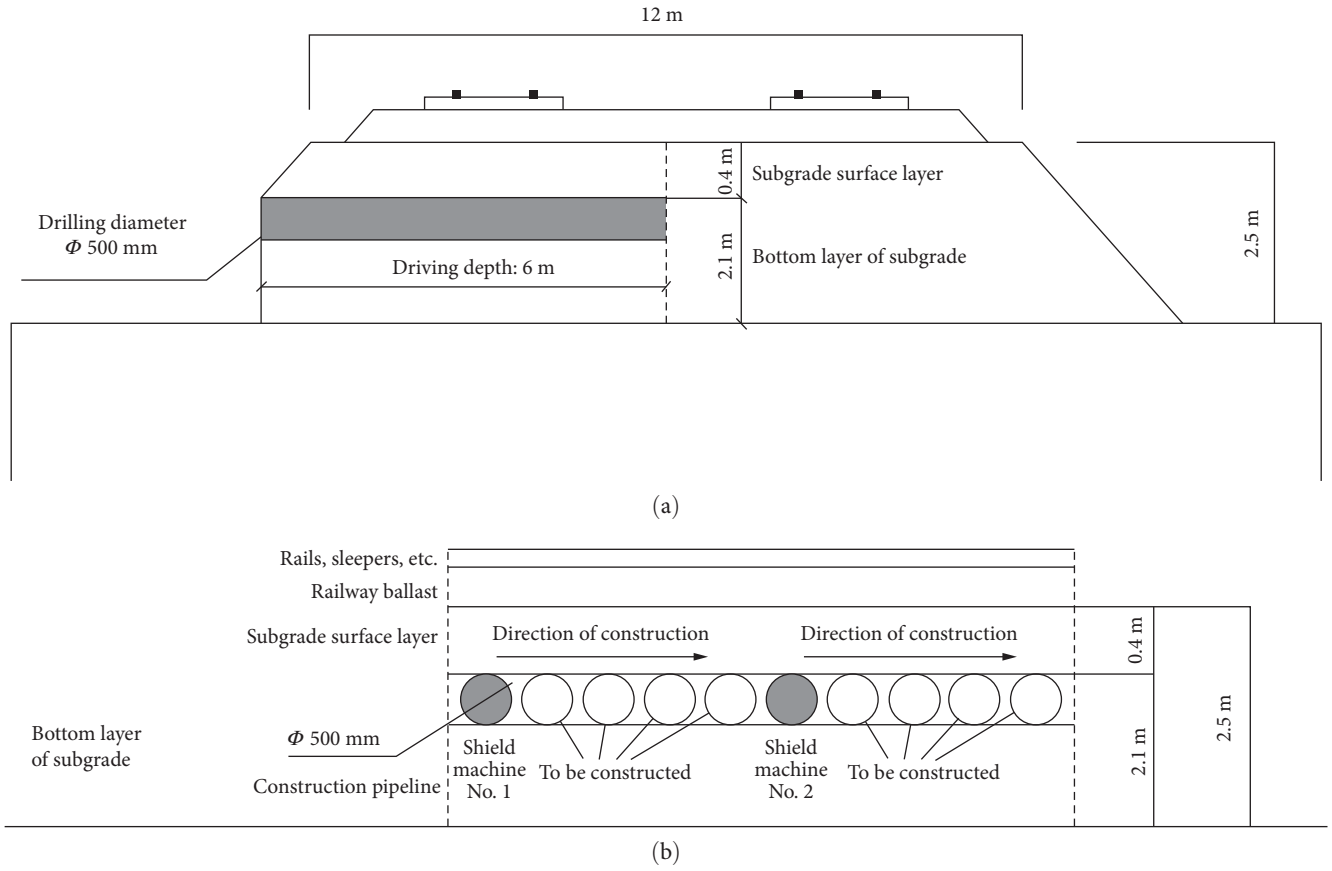

Figure 2: Microshield construction section: (a) cross-section and (b) profile.

(a) (b)

Figure 3: Field shield segment: (a) PE tube and (b) steel pipe.

the number of boreholes was 10, the net distance between the two boreholes was 100 mm, and the range involved was 500 mm × 10 + 100 mm × 10 = 6 m. The results of grid division and various structural parameters are shown in Figure 7 and listed in Table 3 [15–19]. Referring to the study on the interaction between pipeline and soil by researchers at home and abroad [20, 21], this paper uses the life–death element method to bind the inner surface of soil to the outer surface of pipeline during shield tunneling.

4.1.1. Verification of the Steel Pipe Construction Model. The construction section K200 + 367.6–K200 + 397.6 was selected as the research object. To verify the validity of the calculated finite-element model, the measured settlement value of the construction site line of this section was compared with the numerical value, as shown in Figure 8. When simulating the steel pipe shield, the settlement data were similar, indicating that the model effectively reflected the actual settlement state of the steel pipe shield.

Table 2: Physical and mechanical parameters of Xining–Geermu Railway bed fillers.

Filling properties	Measured value
Specific gravity of soil particles (G)	2.70
Density (kg/m^3)	2300
Moisture content (%)	25–40
Cohesion (kPa)	40
Internal friction angle (°)	18
Modulus of elasticity (MPa)	30
Poisson's ratio per μ	0.20

(a) (b) (c)

Figure 4: Actual layout of survey points: (a) rail waist; (b) electrified uprights; and (c) schematic diagram of a microprism.

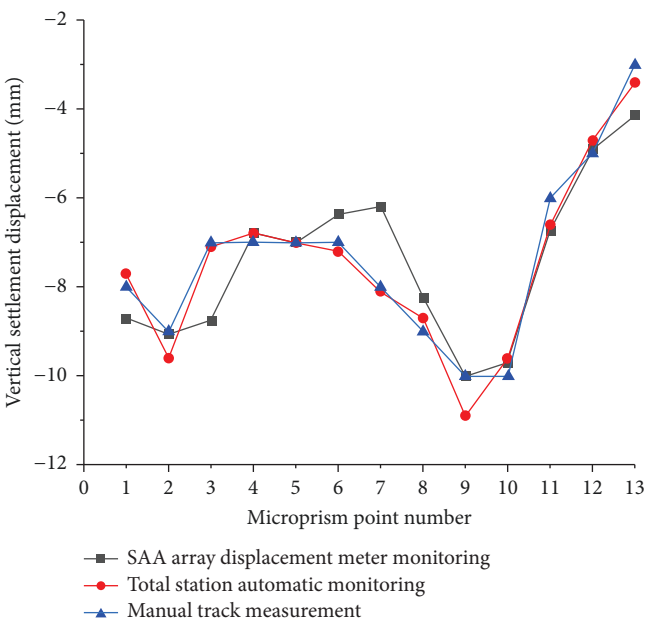

Figure 5: Comparison of the results of various measurement methods in the test section.

4.1.2. Verification of the PE Tube Construction Model. In the PE tube construction section, due to the small elastic modulus and soft material of the PE tube, there is formation loss and deformation caused by OD in site construction. Du et al. [22] adopted two tunnel contraction boundary conditions of uniform contraction and nonuniform contraction to simulate tunnel excavation, as shown in Figure 9. As the maximum surface settlement curve of working condition B was close to the measured value, this paper adopted the boundary conditions of working condition B for finite element analysis (FEA).

Loganathan and Poulos [23] provided the equivalent of the formation movement characteristics around the tunnel with the nonuniform radial movement model. They proposed the calculation theory of replacing formation loss parameters with the formation loss function and derived the tunnel diameter reduction parameters as follows:

$$\varepsilon_0 = \frac{\pi\left(r + \frac{g}{2}\right) - \pi r^2}{\pi r^2} \times 100\% = \frac{4gr + g^2}{4r^2} \times 100\%, \quad (1)$$

$$g = 2r\left(\sqrt{1 + \varepsilon_0} - 1\right), \quad (2)$$

where r is the outer diameter of the segment; ε_0 is the soil loss ratio; and g is the clearance parameter.

Peck [24] proposed a method to estimate the ground settlement caused by tunnel excavation. Based on the theoretical analysis and field observation data, Attewell [25] introduced the curve of the subgrade surface lateral settlement trough into three-dimensional (3D) space and derived Formula (3) for calculating 3D shield settlement:

(a) (b)

Figure 6: The construction difference between the two segments: (a) steel pipe segments and (b) PE tube segments.

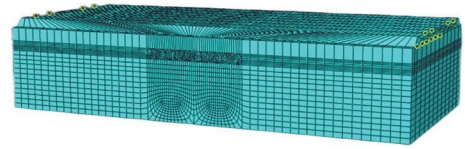

Figure 7: ABAQUS finite-element model mesh.

Table 3: Material parameters of each structure.

Structure	Density (kg/m^3)	Modulus of elasticity, E (MPa)	Poisson's ratio μ
Ballast	2,200	700	0.26
Base bed filler	2,300	30	0.2
Concrete	2,100	34,500	0.25
Steel pipe	7,850	210,000	0.25
PE tube	2,000	1.07	0.41

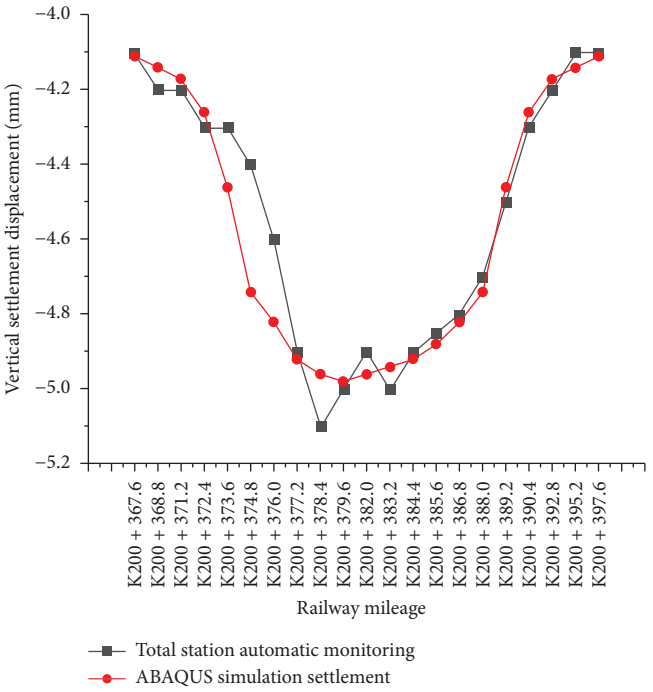

Figure 8: ABAQUS simulation of settlement using steel tube segments was compared with actual monitoring.

$$V = \frac{S_A}{S_D} = \frac{\int_a^b S(x)dx}{\pi D^2/4}, \tag{3}$$

where V is the formation loss rate, S_A is the area of the surface settlement trough, S_D is the tunnel excavation area, $S(x)$ is the surface settlement trough curve, and D is the diameter of the tunnel excavation face.

The actual overburden area of the shield is equivalent to the surface settling trough area. Therefore, the proposed excavation area of the shield was equivalent to the excavation area of the tunnel. The OD radius of the in situ shield drilling was 20 mm, the formation loss rate V was 14.3%, so the equivalent soil loss ratio was also estimated as 14.3%. To simplify the calculation, it was approximated that the formation loss rate remained unchanged in the construction process. The comparative analysis of the measured and simulated value showed, as seen in Figure 10, their consistency in value and phase, indicating that the model effectively reflected the actual settlement state of the PE tube shield. The reason for the bulge in the center of the settlement curve was that the shield construction was similar to the construction of a double tunnel with a relatively close distance, and the settlement curves were superimposed on each other, resulting in a

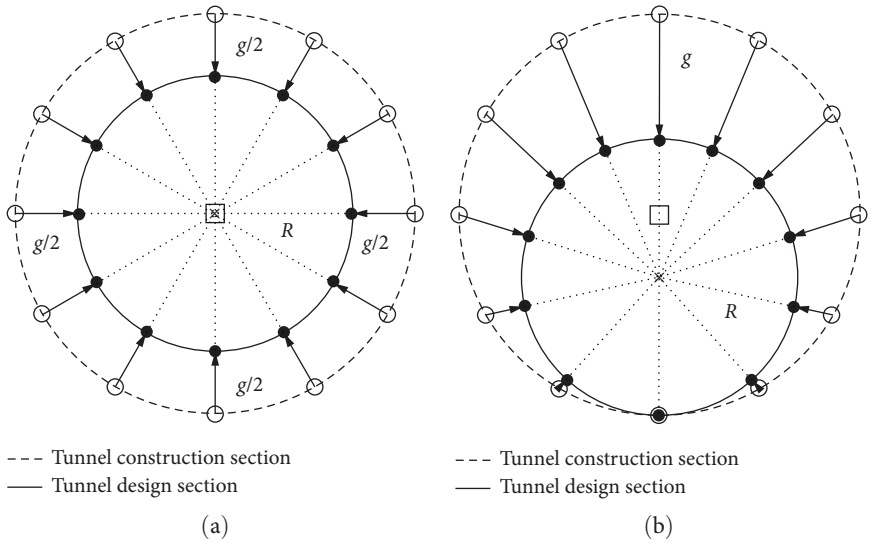

Figure 9: Displacement boundary conditions of the tunnel section: (a) with uniform contraction; (b) with nonuniform contraction. Dashed lines correspond to tunnel construction section and solid lines to tunnel design section.

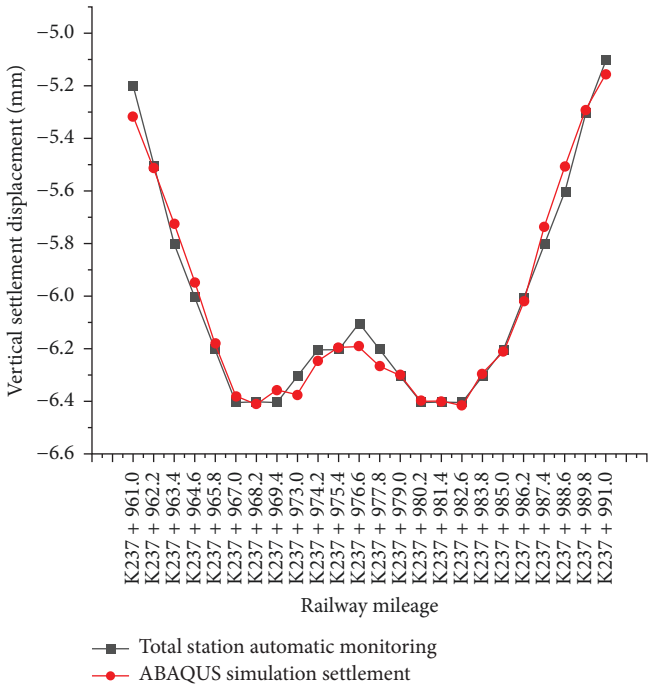

Figure 10: ABAQUS simulation of settlement using PE tube segments was compared with actual monitoring.

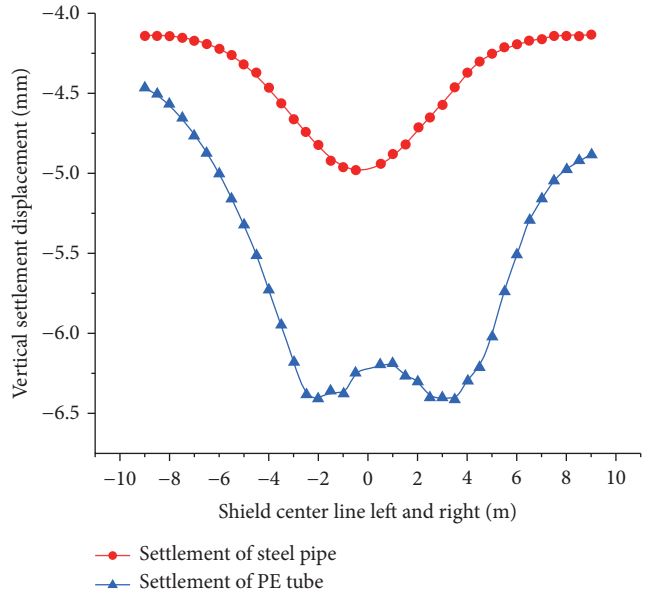

Figure 11: Effect of shield segments with different materials on subgrade surface settlement.

settlement curve similar to that of a double-hole parallel tunnel [26].

5. Analysis of Subgrade Settlement and Deformation

5.1. Effect of Segment Material on Settlement Deformation. To select an economical and reasonable shield segment material, the shield segment was subdivided into rigid and flexible segments, and steel pipes and PE tubes were selected for the simulation analysis. The resulting settlement is shown in Figure 11. When steel pipe segments were used for construction, the line settlement was the smallest, and the maximum settlement was 4.98 mm, meeting the safety requirements of the railway operation. However, the price of steel pipes was higher than that of PE tubes, and on-site construction required many pipe segments. The project cost would be significantly increased if steel pipes were used in the rectification range of frost heave defects in the Xige Line. Therefore, from an economic point of view, this study focused on PE tubes' application to microshields and construction process optimization so that the settlement of the line was controlled within 6 mm.

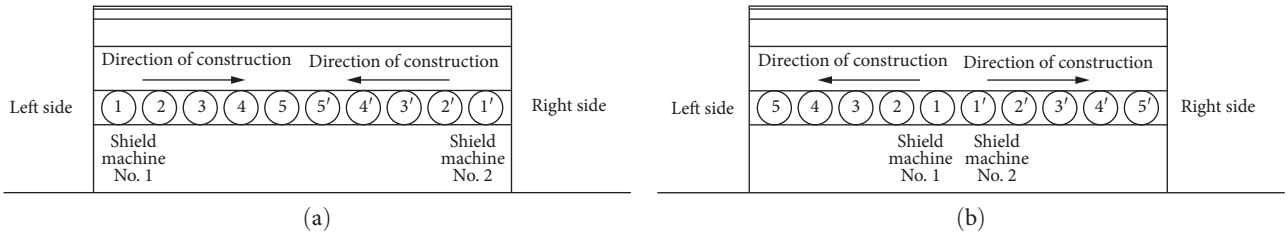

Figure 12: Different construction sequences: (a) from the middle to the sides and (b) from the sides to the middle.

Table 4: Construction conditions of different lateral directions and different directions.

Segment material	Construction order	Construction condition
Steel pipe	From the sides to the middle	Condition 1
Steel pipe	From the middle to the sides	Condition 2
PE tube	From the sides to the middle	Condition 3
PE tube	From the middle to the sides	Condition 4

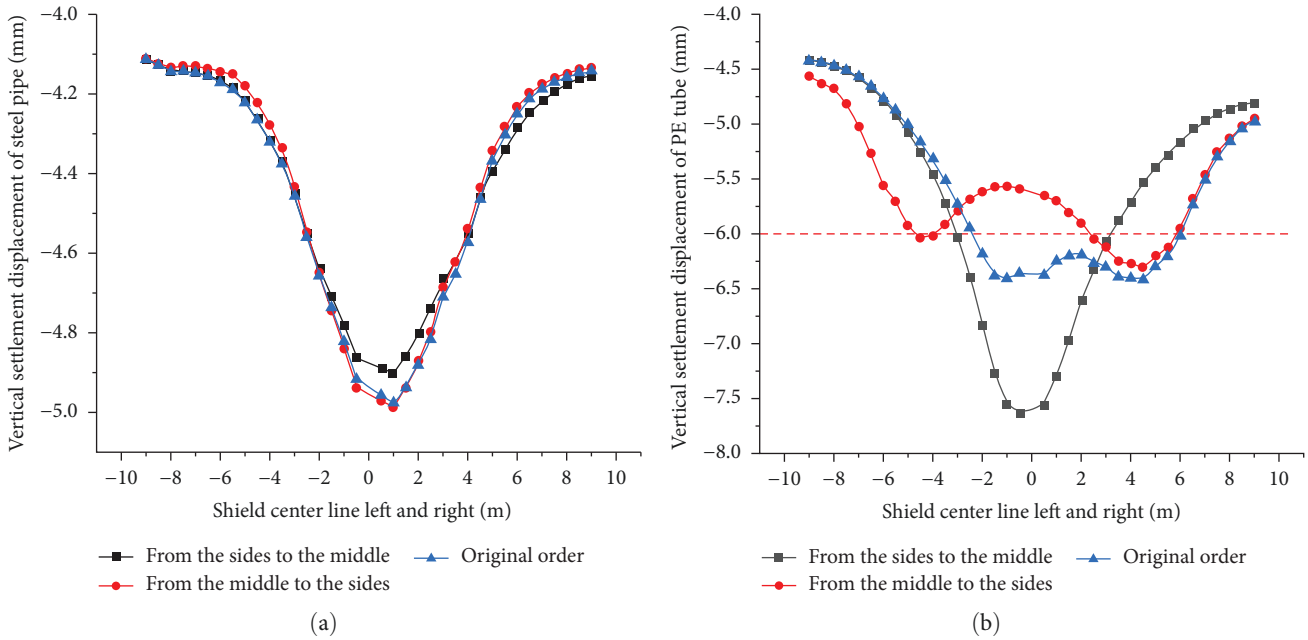

Figure 13: Effect of segment material and construction sequence on settlement deformation of subgrade surface: (a) steel pipe and (b) PE tube.

5.2. Effect of the Construction Process on Line Settlement and Deformation. This paper simulated the effect of the construction process on settlement, aiming to reduce the settlement of the line by optimizing the construction process. The original construction process of the site was four times the diameter of the pipe with the same direction on one side. The model simulation of different construction processes was carried out to with the purpose of effectively controlling the settlement of the line and optimizing the construction technology of the microshield under different working conditions.

5.2.1. Effect of Construction Sequence on Line Settlement and Deformation. To clarify the effect of different construction sequences on settlement deformation, each pipeline was numbered according to the construction sequence, and different construction sequences were adopted, as shown in Figure 12. Each working condition in Table 4 was simulated, with the settlement results depicted in Figure 13. It can be seen from the analysis that for steel pipe construction, the line settlement caused by working condition 1 was the least. The reason was that when the construction occurred from the middle to the two sides, the pipeline near the centerline was excavated preferentially, and the deformation lasted the longest, so the line settlement was larger. For PE tube construction, the line settlement was the least in working condition 4 because when shield construction was carried out from the center to both sides, the central soil was replaced with high-stiffness concrete, constraining the vertical deformation

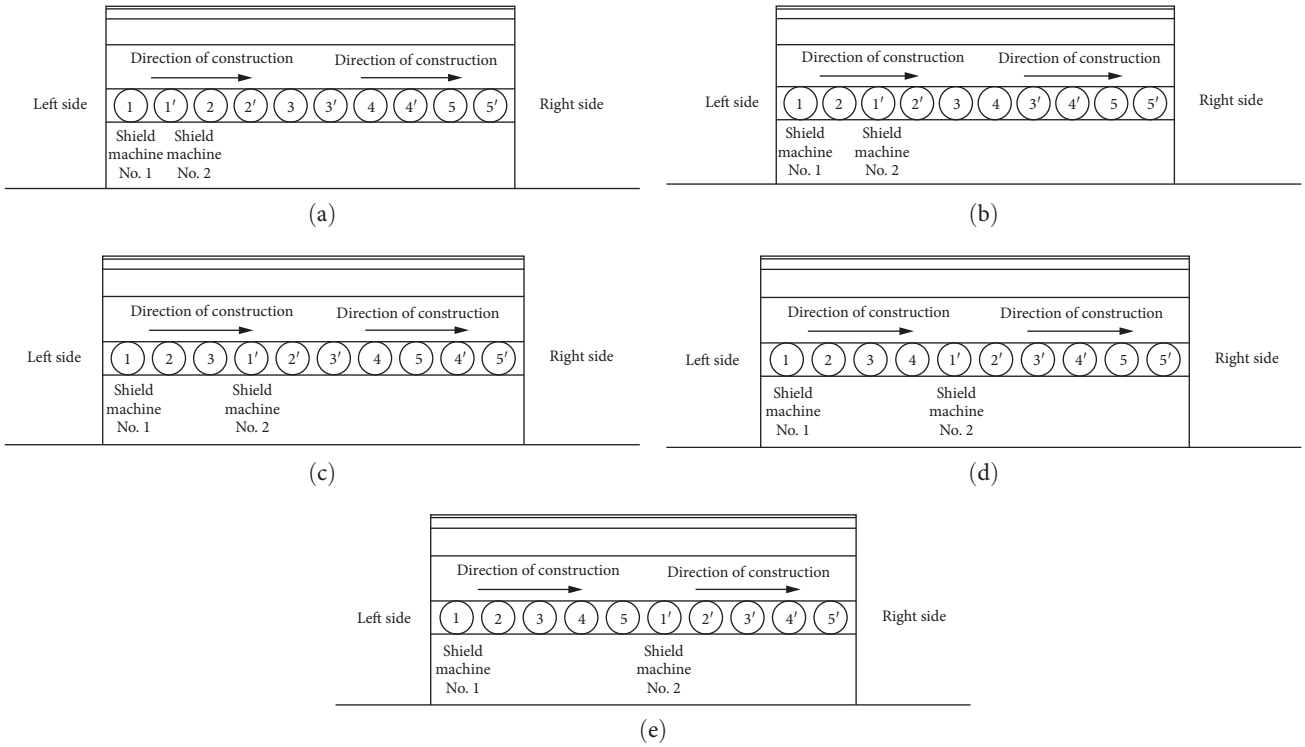

Figure 14: Construction conditions with various interval-to-pipe diameter ratios: (a) 0; (b) 1; (c) 2; (d) 3; and (e) 4.

Table 5: Construction conditions with different pipe diameter intervals.

Segment material	Interval-to-pipe diameter ratio	Construction sequence	Construction condition
Steel pipe	0	One side in the same direction	Condition 5
Steel pipe	1	Ditto	Condition 6
Steel pipe	2	Ditto	Condition 7
Steel pipe	3	Ditto	Condition 8
Steel pipe	4	Ditto	Condition 9
PE tube	0	Ditto	Condition 10
PE tube	1	Ditto	Condition 11
PE tube	2	Ditto	Condition 12
PE tube	3	Ditto	Condition 13
PE tube	4	Ditto	Condition 14

of the soil caused by excavation and reduced the soil settlement and deformation at the center of the replacement backing structure. For shield construction on both sides toward the center, the settlement curves of the line affected each other, resulting in continuous deformation and settlement of the soil in the centerline of the shield, and settlement control in the line center was not realized until the later step. Therefore, the center settlement of the line in working condition 3 was large.

5.2.2. Effect of Construction Interval on Settlement Deformation. To clarify the effect of different construction intervals on settlement deformation, each pipe was numbered according to the sequence of construction; the direction of construction was kept unchanged, and only the interval of drilling segments was changed, as shown in Figure 14. Each working condition in Table 5 was simulated, as shown in Figure 15.

For steel pipe construction, the line settlement in working condition 5 was the least. The line settlement in working condition 12 was the least for PE tube construction. With the increased diameter of the interval pipe, the settlement first decreased and then increased because the construction of two shield tunneling machines was similar to that of double parallel tunnels. The surface settlement curve was unimodal at a small distance between the two pipes. When the spacing (interval) expanded to a certain value, the shape of the surface settlement curve changed from a single peak to a double peak. When the spacing was further expanded, the surface settlement curve featured double peaks [27]. When the interval was two times the diameter of the pipe, after the

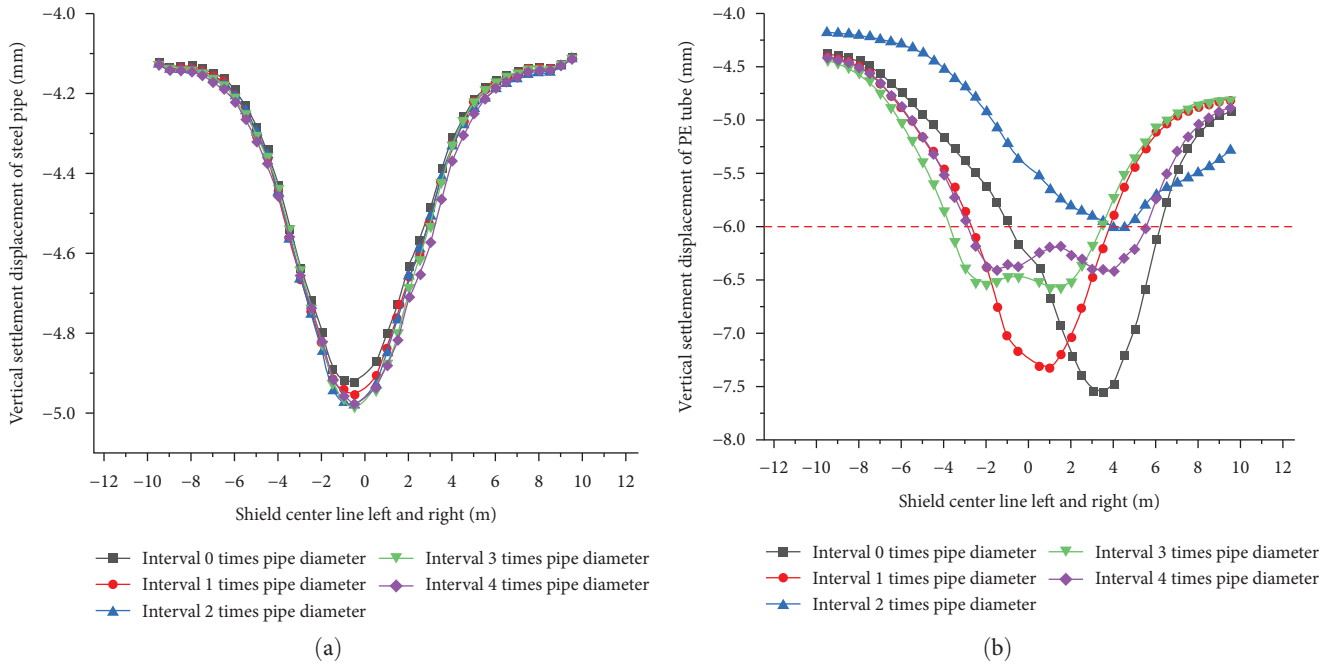

Figure 15: Effect of segment material and construction interval on settlement deformation of subgrade surface: (a) steel pipe and (b) PE tube.

Table 6: Effect of typical working conditions on settlement deformation of transmission line.

Segment type	Interval-to-pipe diameter ratio	Construction sequence	Construction condition	Maximum line settlement in shield center (mm)
Steel pipe	0	One side in the same direction	Condition 5	4.92
Steel pipe	2	From the sides to the middle	Condition 1	4.90
PE tube	2	One side in the same direction	Condition 12	6.0
PE tube	2	From the middle to the sides	Condition 4	6.3

completion of the first round of pipe segment construction, the second round of grouting made up for the formation loss caused by the previous round of pipe excavation in time. After concrete grouting, the restraining effect on the soil controlled the subgrade subsidence of the upper part of the pipe segment promptly, so the settlement of the line was minimal. For the construction with an interval of zero and one pipe diameter, the settlement curve had still a single peak, similar to the construction of a single large-diameter pipe, and the settlement was larger. For the construction with an interval of three and four pipe diameters, the soil deformation could not be controlled by grouting in time, and the settlement was still larger.

By comparing the maximum settlement value near the center of the subgrade surface generated under various working conditions in Tables 4 and 5, the working condition with the maximum settlement in the center of the line was further regarded as a typical working condition, as shown in Table 6. When steel pipes were used for construction, the settlement of working condition 1 was the lowest. When PE tubes were used for construction, the settlement of working condition 12 was the lowest, and the maximum settlement was controlled within 6 mm, meeting the requirements of settlement control for safe railway operation.

5.2.3. Effect of Formation Loss on Line Settlement and Deformation. When using a PE tube sheet for shield construction, the formation loss was large due to the small stiffness and soft material of the PE tube. According to the above calculation, when the excavation section was expanded to 20 mm, the formation loss rate was 14.3%. Currently, the control overcutting range was 15, 10, 5, and 0 mm, and the formation loss rates were 11%, 7.5%, 3.9%, and 0%, respectively, according to Formula (3). FEA was carried out on the loss rates of different strata, as shown in Figure 16. The formation loss and maximum settlement were separately analyzed and fitted, as shown in Figure 17. There was a linear correlation between the maximum settlement and formation loss, with the following fitting equation: $y = -8.9415 - 5.1028x$. At a formation loss rate of −10.03%, the maximum settlement of the line was 6 mm. Therefore, if the technology of PE tube construction was improved, and the formation loss

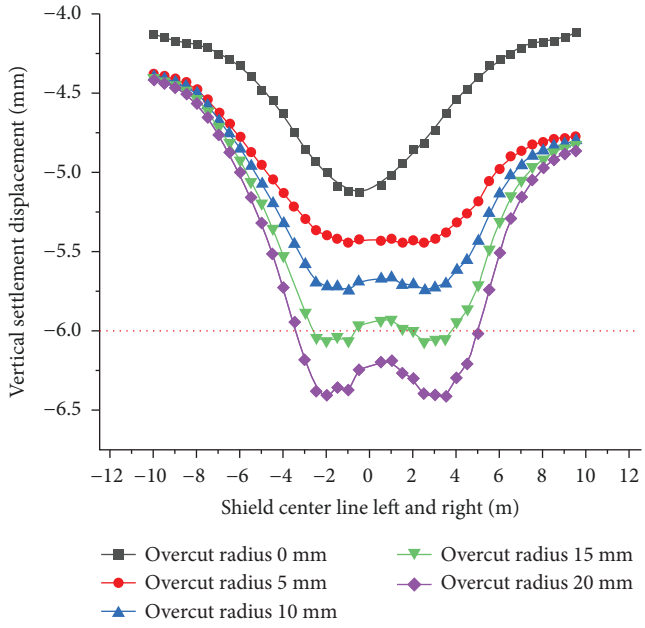

Figure 16: Vertical settlement displacement of the subgrade surface layer with account of ground loss effect in the construction of the PE segment shield machine.

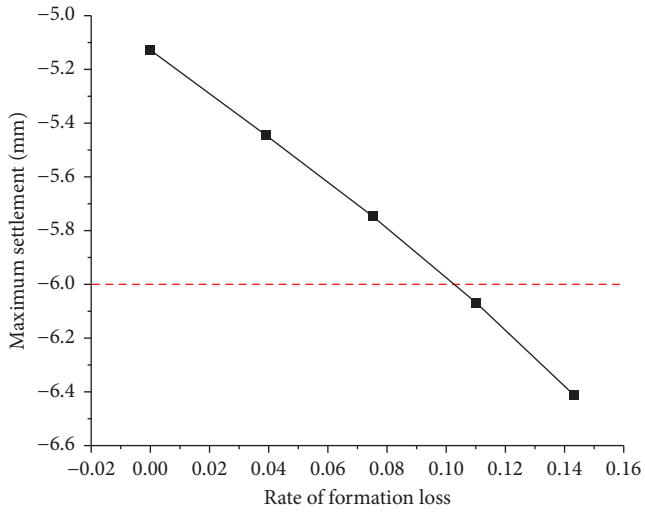

Figure 17: Variation of the PE segment maximum settlement with the formation loss rate.

was controlled within 10%, the line settlement generated by PE tube shield construction could be less than 6 mm, meeting the settlement control requirements of railway safety operation.

6. Conclusions

(1) The performed numerical analysis of microshield segments made of different materials revealed that steel pipes used in the shield segment provided a smaller line settlement than PE tubes. Still, the steel pipe has the disadvantages of high price and poor economy when used in large quantities. Using a PE tube as the shield segment produces a larger line settlement but is more cost-effective.

(2) The settlement generated by the construction process occurring from both sides to the middle was minimal when steel pipe segments were used. When PE tubes were used for construction, the settlement generated by the construction process with a unilateral direction interval of two times the pipe diameter was the least.

(3) When PE tubes were used in the microshield construction segment, the surface settlement curve exhibited the following behaviors for the different segment intervals: when the shield pipe interval was two times the pipe diameter or less, the surface settlement curve was unimodal; when the shield pipe interval was three times the pipe diameter or above, the surface settlement curve featured double peak.

(4) According to the analysis of the formation loss rate generated during construction, when using PE tubes as shield segments, the overdigging range should be controlled, and the formation loss rate should be controlled within 10%.

Data Availability

No data were used to support the findings of this study.

Conflicts of Interest

The authors declare that they have no conflicts of interest.

Acknowledgments

The study is supported by the Science and Technology Research and Development Program of China National Railway Group Co., Ltd. (P2021G047), and Science and Technology Project Plan of Hebei Transportation Department (202304202306).

References

[1] H. Cui, W. Wang, L. Yan, Z. Zhang, B. Shao, and C. Zhu, "Durability of stabilised coarse-grained soil as fill material for high-speed rail subgrade in seasonally frozen regions," *Journal of Railway Science and Engineering*, vol. 18, no. 9, pp. 2225–2233, 2021.

[2] N. Yang, "Analysis on railway subgrade frost damage in the Xining-Geermu section of Qinghai–Tibet railway in Qinghai lake seasonal frozen soil region," *Railway Construction Technology*, vol. 12, no. 6, pp. 96–98,119, 2017.

[3] Y. Wang, *Study on frost heave characteristics and treatment methods of subgrade in seasonal frozen soil area*, M. A. Thesis, Lanzhou Jiaotong University, China, 2018.

[4] B. Tai, Z. Yue, T. Sun, S. Qi, L. Li, and Z. Yang, "Novel anti-frost subgrade bed structures a high speed railways in deep seasonally frozen ground regions: experimental and numerical studies," *Construction and Building Materials*, vol. 269, Article ID 121266, 2021.

[5] Y.-P. Sheng, Z.-H. Da, Z.-R. Yue, and Y.-H. Tian, "Experimental research on the stability of embankment-

bridge transition section of high-speed railway in seasonal frozen regions," *Journal of Railway Engineering Society*, vol. 35, no. 1, pp. 17–22, 2018.

[6] T. Hu, J. Liu, and Z. Yue, "Study on solar active heating device for subgrade in seasonally frozen soil region," *China Railway Science*, vol. 42, no. 2, pp. 39–49, 2021.

[7] T. Hu, J. Liu, Z. Yue, L. Xu, and Z. Zhang, "Proposed application of a geothermal heat pump technique to address frost damage of embankments in cold regions," *Cold Regions Science and Technology*, vol. 195, Article ID 103474, 2022.

[8] X. Li, *Research on prevention and treatment measures of freeze-heave fluid-thermal coupling of subgrade in cold region*, M. A. Thesis, Southwest University of Science and Technology, China, 2022.

[9] X. Liu, Z. Yue, and T. Hu, "Study on effect of frost heaving suppression of new type of thermal insulation strengthening layer for high-speed railway subgrade in cold region," *Journal of the China Railway Society*, vol. 44, no. 2, pp. 108–116, 2022.

[10] W. Yang, "Feasibility test investigation on remediation of railway roadbed seasonal frost damage by salt injection method," *Science Technology and Engineering*, vol. 19, no. 10, pp. 204–209, 2019.

[11] H. Yan, "Target replacement remediation technology for railway subgrade frost-heaving by micro-shield in cold region," *Railway Engineering*, vol. 59, no. 6, pp. 93–96, 2019.

[12] Y. Zhang, "Construction technique on replacement of frost damage subgrade by mini-shield for operating railway," *Railway Engineering*, vol. 59, no. 3, pp. 76–79, 2019.

[13] Y. Wang, X. Wang, N. Yang, Yu Wang, and Y. Zhang, "Field test study on railway subgrade against frost damage in seasonally frozen ground areas by using salt injection method," *Journal of Glaciology and Geocryology*, vol. 39, no. 6, pp. 1265–1272, 2017.

[14] Z. Yue and S. Jie, "Research on the line smoothness monitoring technology of subgrade grouting of high-speed railway in operation period," *Journal of Railway Engineering Society*, vol. 1, no. 280, pp. 13–17,32, 2022.

[15] J. Feng, *Discrete element analysis and experimental verification of railway ballast mechanical characteristics*, M. A. Thesis, Dalian University of Technology, China, 2017.

[16] W. Zhao, *Stability study and engineering treatment analysis on embankment upon the slope at ando section in the permafrost of Qinghai–Tibet railway*, M. A. Thesis, Beijing Jiaotong University, China, 2008.

[17] Ministry of Housing and Urban–Rural Development of the People's Republic of China, *Code for Design of Concrete Structures GB50010-2010*, China construction industry press, Beijing, 2010.

[18] Ministry of Housing and Urban–Rural Development of the People's Republic of China, *Standard for Design of Steel Structures GB50017-2017*, China construction industry press, Beijing, China, 2017.

[19] China State Administration of Technology and Quality Supervision, *China State Administration of Technology and Quality Supervision GB/T 13663-2000*, China State Administration of Technology and Quality Supervision, Beijing, China, 2000.

[20] T. Li, W. Zhao, R. Liu, J.-Y. Han, P. Jia, and C. Cheng, "Visualized direct shear test of the interface between gravelly sand and concrete pipe," *Canadian Geotechnical Journal*, vol. 4, Article ID 2022-0007, 2023.

[21] J. Han, J. Wang, D. Jia et al., "Construction technologies and mechanical effects of the pipe-jacking crossing anchor-cable group in soft stratum," *Frontiers in Earth Science*, vol. 10, Article ID 1019801, 2023.

[22] Z.-L. Du, M.-S. Huang, and Z. Li, "DCM-based on ground loss for response of group piles induced by tunneling," *Rock and Soil Mechanics*, vol. 30, no. 10, pp. 3043–3047, 2009.

[23] N. Loganathan and H. G. Poulos, "Analytical prediction for tunneling-induced ground movements in clays," *Journal of Geotechnical and Geoenvironmental Engineering*, vol. 124, no. 9, pp. 846–856, 1998.

[24] R. Peck, "Deep excavation and tunneling in soft ground," *7th International Conference on Soil Mechanics and Foundations Engineering*, vol. 7, no. 3, pp. 225–231, 1969.

[25] P. Attewell, "Engineering contract, site investigation and surface movements in tunneling works," *Soft Ground Tunneling*, vol. 42, no. 2, pp. 4–12, 1981.

[26] B. Liu, L. Tao, C. Ding, H. Li, Q. Pan, and X. Gao, "Prediction for ground subsidence induced by subway double tube tunneling," *Journal of China University of Mining and Technology*, vol. 35, no. 3, pp. 356–361, 2006.

[27] Y.-F. Gong, B. Wang, H.-B. Wei, Z.-H. He, Y.-L. He, and Y.-F. Shen, "Surface subsidence law of double-line shield tunnel based on peck formula," *Journal of Jilin University (Engineering and Technology Edition)*, vol. 48, no. 5, pp. 1411–1417, 2018.